

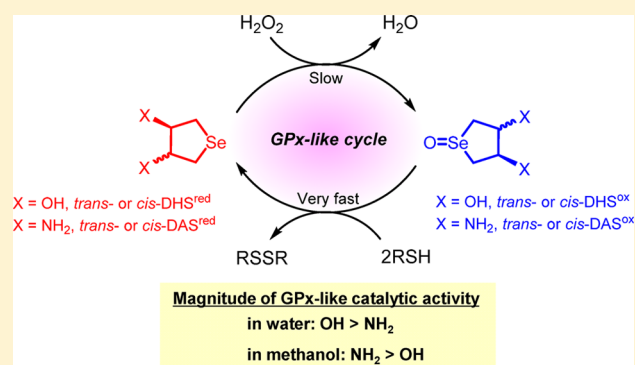
Effects of Ring Size and Polar Functional Groups on the Glutathione Peroxidase-Like Antioxidant Activity of Water-Soluble Cyclic Selenides

Kenta Arai, Fumio Kumakura, Motoi Takahira, Natsumi Sekiyama, Nozomi Kuroda, Toshiki Suzuki, and Michio Iwaoka*

Department of Chemistry, School of Science, Tokai University, Kitakaname, Hiratsuka-shi, Kanagawa 259-1292, Japan

Supporting Information

ABSTRACT: To elucidate the effects of ring structure and a substituent on the glutathione peroxidase- (GPx-) like antioxidant activities of aliphatic selenides, series of water-soluble cyclic selenides with variable ring size and polar functional groups were synthesized, and their antioxidant activities were evaluated by NADPH-coupled assay using H_2O_2 and glutathione (GSH) in water and also by NMR spectroscopy using H_2O_2 and dithiothreitol (DTT^{red}) in methanol. Strong correlations were found among the GPx-like activity in water, the second-order rate constants for the oxidation of the selenides, and the HOMO energy levels calculated in water. The results support the conclusion that the oxidation process is the rate-determining step of the catalytic cycle. On the other hand, such correlations were not obtained for the activity observed in methanol. The optimal ring size was determined to be five. The type of substituent ($\text{NH}_2 < \text{OH} < \text{CO}_2\text{H}$) and the number can also control the activity, whereas the stereoconfiguration has only marginal effects on the activity in water. In methanol, however, the activity rank could not be explained by the simple scenarios applicable in water.

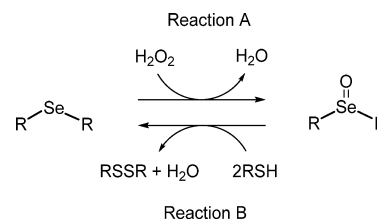


INTRODUCTION

Selenium (Se), a group 16 chalcogen element, is an essential micronutrient for living organisms. Generally, selenium is involved in proteins as selenocysteine (Sec), which is a selenium analogue of the natural amino acid cysteine (Cys) and is genetically coded similarly to other proteinogenic amino acids.¹ Significant roles of selenium-containing proteins are implicated in the maintenance of redox homeostasis in cells. Glutathione peroxidase (GPx), a representative selenoenzyme, catalyzes the reduction of reactive oxygen species (ROS), such as hydrogen peroxide (H_2O_2), to harmless water (H_2O) using glutathione (GSH) as a reducing cofactor.^{2–5} In the past few decades, the synthesis and application of low-molecular-weight organoselenium compounds as possible GPx mimics have been explored in the field of chemical biology.^{6–11} For example, aromatic diselenides (ArSeSeAr) having a polar substituent, such as OH and NH_2 , near the selenium atom can imitate the catalytic cycle of GPx and exhibit significant GPx-like antioxidant activity.^{12–19} For such GPx mimics, selection of a polar substituent is an important factor controlling the activity because the substituent can regulate the reactivity and stability of intermediates appearing during the catalytic cycle through weak nonbonded $\text{Se}\cdots\text{X}$ ($\text{X} = \text{O}, \text{N}$, etc.) interactions and/or inductive electronic perturbations.

On the other hand, monoselenides (RSeR) have less frequently been investigated as potential GPx mimics. However, selenides can be oxidized with H_2O_2 to the corresponding selenoxides, and the selenoxides can be reduced back to the selenides with thiols (RSH). This selenide–selenoxide redox system indeed provides a unique catalytic cycle (Scheme 1)

Scheme 1. GPx-Like Redox Cycle of Selenides



analogous to that of GPx.^{20,21} Rahmanto and Davies investigated the GPx-like activity of selenomethionine to reduce protein hydroperoxides.²² Back et al. reported a high GPx-like activity of bis(3-hydroxypropyl) selenide, which forms a reactive spiro dioxoselenurane species, instead of a selenoxide,

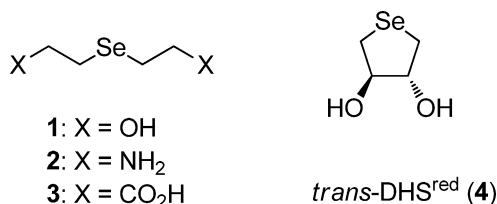
Received: March 11, 2015

Published: May 5, 2015

when oxidized.²³ Nascimento et al. recently characterized, in the oxidation products of aryl benzyl selenides in methanol, a highly reactive hydroxy perhydroxy selenane species [RR'Se(OH)OOH], which would be a key intermediate for the observed significant GPx-like catalytic activity.²⁴

We recently found that the GPx-like antioxidant activity of water-soluble aliphatic selenides having various polar functional groups (X) (Scheme 2) depends critically on X: The activity

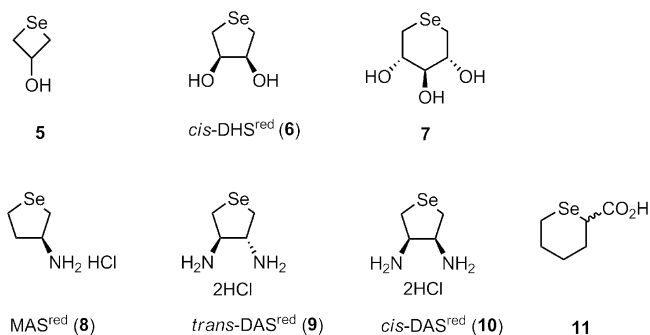
Scheme 2. Water-Soluble Selenides Studied Previously



increases in the order 2 (NH₂) < 1 (OH) < 3 (CO₂H) in aqueous medium, whereas the order is inverted in methanol [i.e., 3 (CO₂H) < 1 (OH) < 2 (NH₂)].²¹ Similar substituent effects were reported for the GPx-like activities of other series of simple aliphatic selenides.²⁵ It was also indicated that the rate-determining step of the catalytic cycle is the oxidation of the selenide (i.e., reaction A in Scheme 1) and that the reduction of the selenoxide (i.e., reaction B in Scheme 1) proceeds rapidly.^{21,26} Furthermore, cyclic selenide 4 (*trans*-DHS^{red})²⁷ exhibits higher GPx-like activity in both water and methanol than open-chain selenide 1. The activity enhancement observed for 4 was attributed to the cyclic structure, which would modify the HOMO so that the oxidation of 4 takes place more effectively.²¹ In this context, cyclic selenides having a polar functional group other than OH would be interesting synthetic targets to enhance the GPx-like activity.

In the present study, to elucidate more clearly the effects of ring structure and polar functional groups on the GPx-like antioxidant activity of selenides, the series of water-soluble cyclic selenides 5–11 (Scheme 3) with variable ring size and

Scheme 3. Water-Soluble Cyclic Selenides Examined in This Study

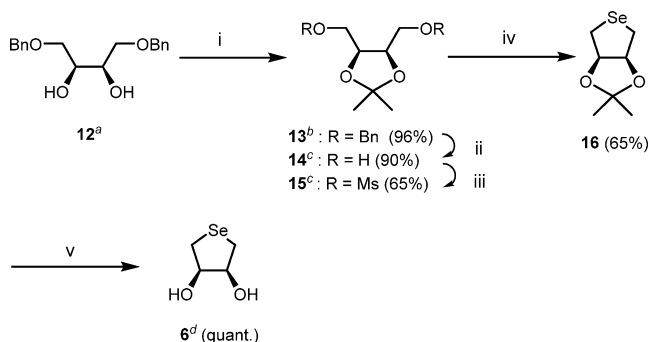


substituents were synthesized, and their redox behaviors were compared with those of 1–4 as reference compounds. The effects of stereoconfiguration (i.e., 4 vs 6 and 9 vs 10) and number of a substituent (i.e., 8 vs 9 or 10), as well as solvent effects, are discussed on the basis of the reducing abilities of the selenides (i.e., the ability as reducing agents) and the HOMO energy levels.

RESULTS AND DISCUSSION

Synthesis of Water-Soluble Cyclic Selenides. Hydroxy-substituted four-membered cyclic selenide 5,²⁸ hydroxyl-substituted six-membered cyclic selenide 7,^{29,30} and carboxy-substituted six-membered cyclic selenide 11²⁰ were synthesized according to the literature procedures. Five-membered cyclic selenide 8 (monoaminoselenolane, MAS^{red}) was obtained as a hydrochloride salt from L-aspartic acid in six steps.³¹ On the other hand, cyclic selenide 6 (*cis*-dihydroxyselenolane, *cis*-DHS^{red}), which corresponds to the *cis* stereoisomer of *trans*-DHS^{red} (4), was synthesized according to Scheme 4. Dibenzyl

Scheme 4. Synthesis of *cis*-DHS^{red} (6)^{a,b}

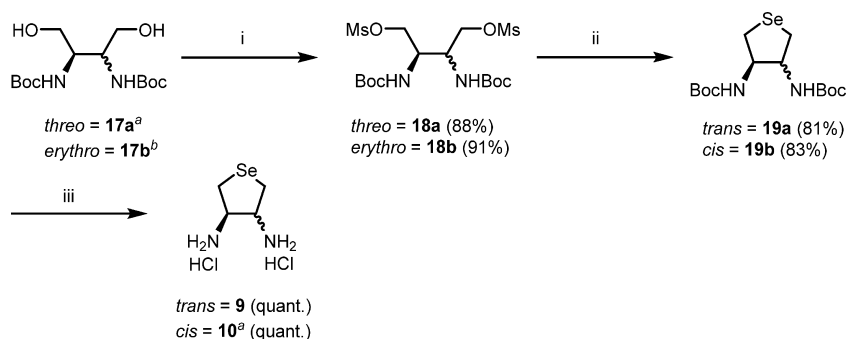


^aReagents and conditions: (i) DMP, *p*-TsOH, acetone, rt, 1.5 h; (ii) H₂, Pd/C, MeOH, rt, 23 h; (iii) MsCl, pyridine, 0 °C, 2.5 h; (iv) NaHSe, EtOH/THF, reflux, 4 h; (v) AcOH, MeOH, reflux, 19 h. ^bSources: (a) Reference 32, (b) Reference 33, (c) Reference 34, (d) Reference 35.

ether 12 was prepared from *cis*-2-butene-1,4-diol in two steps by following the literature procedures.³² After conversion of 12 to an acetonide form (13),³³ the benzylic groups (Bn) were removed reductively. The produced diol 14 was then treated with methanesulfonyl chloride (MsCl) to give dimesylate 15.³⁴ *cis*-DHS^{red} (6) was obtained by selenation of 15 with sodium hydrogen selenide (NaHSe) and subsequent deprotection of the acetonide group. The total yield of 6 from 12 was 37%. *cis*-DHS^{red} (6) is a known compound, but the synthetic route in this study was different from the previous one.³⁵

Diaminoselenolanes *trans*-DAS^{red} (9) and *cis*-DAS^{red} (10), with a five-membered ring structure, were synthesized as dihydrochloride salts according to Scheme 5. Starting from diols 17a and 17b, which were prepared in eight and seven steps, respectively, from *cis*-2-butene-1,4-diol by following the literature procedures,^{36–39} target selenides 9 and 10 were obtained in three steps through mesylation and selenation of the hydroxyl groups and subsequent deprotection of the Boc groups. The total yields of 9 and 10 from 17 were 73 and 85%, respectively. Synthesis of *cis*-DAS^{red} (10) was previously reported,³⁶ but our synthetic route was slightly modified from the previous one. All cyclic selenides (5–11) obtained in this study were unambiguously characterized by ¹H, ¹³C, and ⁷⁷Se NMR spectroscopies and HRMS [atmospheric-pressure chemical ionization (APCI+)] analyses (see the Experimental Section for details).

Redox Properties of Selenides/Selenoxides. To confirm the redox properties of the synthesized cyclic selenides (5–11), the oxidation and subsequent reduction (Scheme 1) were monitored by ⁷⁷Se NMR spectroscopy in D₂O. The spectral changes observed for 9 are shown in Figure 1. When 9

Scheme 5. Synthesis of *cis*- and *trans*-DAS^{red}_{*a,b*}

^aReagents and conditions: (i) MsCl, pyridine, 0 °C, 3.5 h; (ii) NaHSe, EtOH/THF, reflux, 4 h; (iii) HCl, H₂O/THF, 30 °C, 18 h. ^bSources: (a) Reference 36, (b) Reference 39.

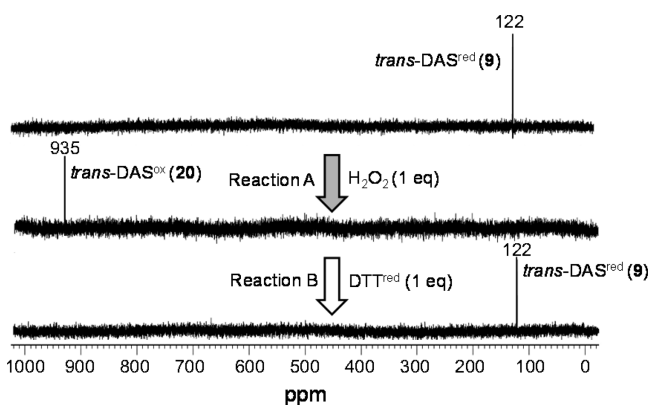


Figure 1. ⁷⁷Se NMR spectral changes upon oxidation (reaction A) and subsequent reduction (reaction B) of *trans*-DAS^{red} (**9**) in D₂O at 25 °C. Reaction conditions were [9]₀ = [H₂O₂]₀ = 48 mM for reaction A, and 1 equiv of DTT^{red} was added for reaction B.

was reacted with 1 equiv of H₂O₂ for 120 min, the absorption for **9** (δ = 122 ppm) completely disappeared, and a new signal that corresponds to selenoxide *trans*-DAS^{ox} (**20**) appeared at δ = 935 ppm. Subsequently, 1 equiv of dithiothreitol (DTT^{red}) was added to the resulting solution as a dithiol substrate to observe the quantitative recovery of **9**. In the ¹H NMR spectrum, the concomitant formation of disulfide DTT (DTT^{ox}) was observed (see ¹H NMR spectra in the Supporting Information). These experiments clearly showed that selenide **9** has the capacity of a redox catalyst as a GPx mimic. The other selenides also showed similar redox behaviors. The ⁷⁷Se NMR chemical shifts observed for the selenides and the corresponding selenoxides are summarized in Table 1. Although all selenides could be transformed quantitatively to selenoxides, the stabilities of the selenoxides varied significantly: *cis*-DHS^{ox} (**26**), **27**, *trans*-DAS^{ox} (**20**), and *cis*-DAS^{ox} (**29**) were stable as solid materials similarly to *trans*-DHS^{ox} (**24**), whereas MAS^{ox} (**28**) gradually decomposed when precipitated from the solution and selenoxides **25** and **30** degraded slowly even in solution upon prolonged preservation. It should be noted that some selenoxides show two absorption signals due to the pyramidalization of the selenoxide moiety.

GPx-Like Antioxidant Activity in Aqueous Medium.

The GPx-like catalytic activities of selenides **5**–**11** in a phosphate buffer solution at pH 7.4 were evaluated at 25 °C by the standard nicotinamide adenine dinucleotide phosphate (NADPH)-coupled method in the presence of glutathione reductase (GR).⁴⁰ In this assay, H₂O₂ is reduced with GSH in

the presence of a catalytic amount of a selenide, and the produced disulfide GSSG is reduced with NADPH by the function of GR enzyme. The speed of H₂O₂ reduction can be monitored by the decreased amount of NADPH, which exhibits UV absorption at 340 nm. Figure 2 shows the decrease of the absorbance at 340 nm as a function of the reaction time. The initial rates (v_0) estimated from Figure 2 are summarized in the second column of Table 2.

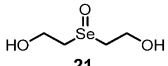
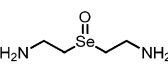
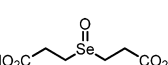
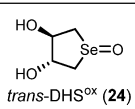
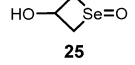
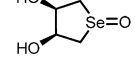
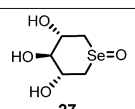
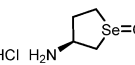
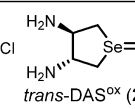
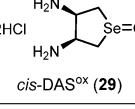
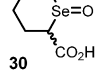
The activities of open-chain selenide **1** and cyclic selenides **4**–**7** are compared in Figure 2A to investigate the effects of ring size on the GPx-like activity. All selenides exhibited a GPx-like activity under the applied conditions, where H₂O₂ was added in excess with respect to NADPH. It is notable that the activities of cyclic selenides **4**–**7** were higher than that of selenide **1**, reconfirming our previous observation that cyclic selenides are more efficient GPx mimics than open-chain selenides.²¹ In addition, the order of the activity, **4** \approx **6** > **5** > **7**, suggested that the optimal ring size for the GPx-like activity of cyclic selenides is five. The relative configuration of the polar substituents (i.e., OH) did not affect the activity because *trans*-DHS^{red} (**4**) and *cis*-DHS^{red} (**6**) showed almost the same activities.

Figure 2B compares the GPx-like activities of **2**–**4** to those of **8**–**11**. As observed for the OH substituent, the GPx-like activities of cyclic selenides **8**–**10** were higher than that of open-chain selenide **2** when the substituent was NH₂. However, in the case of CO₂H, the activity of six-membered cyclic selenide **11** was similar to or slightly lower than that of open-chain **3**, probably because of the lower number of CO₂H groups present in **11**, in addition to the nonoptimal ring size.

In the meantime, in terms of the effects of the functional group, the activities of the cyclic selenides increased in the order **9** and **10** (NH₂ \times 2) < **4** (OH \times 2) < **8** (NH₂ \times 1) < **11** (CO₂H \times 1). This order is almost consistent with that observed for open-chain selenides in aqueous medium, namely, **2** (NH₂) < **1** (OH) < **3** (CO₂H).²¹ Generally, it can be assumed that a negatively charged carboxylic group (–CO₂[–]) at pH 7.4 would enhance the reducing ability of the selenide moiety through inductive electron release, whereas a positively charged amino group (–NH₃⁺) would diminish the reducing ability through inductive electron withdrawal. Therefore, the trend observed for the cyclic selenides can be explained by this simple consideration, except for the case of MAS^{red} (**8**). The reason for the unusual redox behavior of **8** is not clear at this moment.

GPx-Like Antioxidant Activity in Methanol. The activity was evaluated by applying the NMR method as described previously.²⁰ The redox reaction between H₂O₂ and DTT^{red}

Table 1. ^{77}Se NMR Chemical Shifts of Selenides and Corresponding Selenoxides

Selenides	δ_{Se}^a	Selenoxides	δ_{Se}^a
1	80	 21	838
2	78	 22	872
3	179	 23	865
4	74	 <i>trans</i> -DHS ^{ox} (24)	926
5	26	 25	799 (major) and 850
6	84	 <i>cis</i> -DHS ^{ox} (26)	923 (major) and 925
7	80	 27	829
8	135	 MAS ^{ox} (28)	945 and 958 (major)
9	122	 <i>trans</i> -DAS ^{ox} (20)	935
10	128	 <i>cis</i> -DAS ^{ox} (29)	930 and 970 (~1:1)
11	250	 30	753

^a ^{77}Se NMR chemical shifts in D_2O .

was initiated by the addition of H_2O_2 to a solution of DTT^{red} in CD_3OD containing a catalytic amount of a selenide. The reaction progress was monitored by ^1H NMR spectroscopy at 25°C . The relative populations of DTT^{red} and DTT^{ox} were estimated by integration of the peaks at $\delta = 2.63$ and 3.67 ppm for DTT^{red} and at $\delta = 2.87$, 3.03 , and 3.49 ppm for DTT^{ox} . The remaining amounts of DTT^{red} are plotted in Figure 3 as a function of reaction time. The times required for 50% conversion of DTT^{red} to DTT^{ox} in CD_3OD (t_{50}) are summarized in the third column of Table 2.

In methanol, all selenides exhibited GPx-like antioxidant activity as in a phosphate buffer (i.e., in water), but the activity was markedly enhanced in methanol compared to the blank. It is also obvious that the activity varied significantly depending

on the structure and the substituents. When cyclic selenides **4**–**7** are compared to open-chain selenide **1** (Figure 3A), it can be seen that the activities of five-membered ring selenides **4** and **6** are higher than that of **1**, whereas the activity of four-membered ring selenide **5** is nearly equal to that of **1**, and for the six-membered ring selenide **7**, it is even lower. The trend of the activities observed for the cyclic selenides is similar to that observed in water, indicating that the effect of ring size on the GPx-like activity of cyclic selenides is not affected by the solvent (i.e., the optimal ring size is five). However, including open-chain selenide **1**, the order of activity in methanol (i.e., $7 < 1 \approx 5 < 4 < 6$) is significantly different from that observed in water (i.e., $1 < 7 < 5 < 4 \approx 6$). Moreover, for the stereoconfigurations of the two OH substituents (i.e., **4** vs **6**), the effect is striking in methanol. This is in large difference from the marginal effect observed in water. Thus, the effect of solvent is an important factor that can control the relative GPx-like activities of selenides.

In Figure 2B, the GPx-like activities of selenides **2**–**4** and **8**–**11** are compared to investigate the effect of the substituents on the activity. For the selenides with two functional groups, the activity increases in the order $3 (\text{CO}_2\text{H} \times 2) < 10 (\text{NH}_2 \times 2) < 4 (\text{OH} \times 2) < 2 (\text{NH}_2 \times 2) < 9 (\text{NH}_2 \times 2)$, showing that the substitution of the acidic functional groups (CO_2H) by neutral (OH) or basic (NH_2) ones enhances the activity in methanol. In general, the substituent effect on the GPx-like activity in methanol is inverted from that in water,²¹ because the substituent is protonated or deprotonated in water whereas it exists as an electronically neutral form in methanol. Comparison of the activity between **4** and **10**, however, shows a contradiction of this general assumption. Regarding the effect of cyclization, it seems that the ring structure basically increases the activity, according to a comparison of the activities of **2** ($\text{NH}_2 \times 2$) and **9** ($\text{NH}_2 \times 2$). However, **10** ($\text{NH}_2 \times 2$) and **8** ($\text{NH}_2 \times 1$), with five-membered ring structures, showed lower activity than open-chain selenide **2**. Moreover, cyclic diaminoselenolane with the *trans* configuration (**9**) exhibited a higher activity than the *cis* isomer (**10**) in methanol. This trend is opposite to the case of DHS (i.e., **4** vs **6** in methanol). These results strongly suggest that the stereoconfiguration and number of NH_2 substituents have more complex effects on the GPx-like activity in methanol than in water. For the CO_2H substituent, on the other hand, the activity of **3**, with a linear structure, is slightly higher than that of **11**, with a six-membered ring. This trend is consistent with that observed in water.

Based on the overall results obtained from the assays in water and in methanol, it is obvious that the effects of substituents, including number and stereoconfiguration, on the GPx-like antioxidant activities of selenides in methanol are significantly different from those in water. This suggests the possibility that the activity can be controlled by changing the solvent.

Competition of the Reducing Abilities of Selenides.

Because the rate-determining step in the GPx-like catalytic cycle of a selenide is the oxidation process with H_2O_2 to the selenoxide (i.e., reaction A in Scheme 1),²¹ the reducing abilities of selenides should have a strong correlation with the GPx-like activity. To confirm this hypothesis, the competitive oxidations of the selenides with H_2O_2 in D_2O were monitored by ^{77}Se NMR spectroscopy. When selenides **4** and **5** were simultaneously oxidized with 1 equiv of H_2O_2 (Figure 4A), about 80% of the **4** disappeared, and the signal corresponding to the selenoxide (*trans*-DHS^{ox}, **24**) appeared at low magnetic field, whereas the concentration of **5** decreased by only about

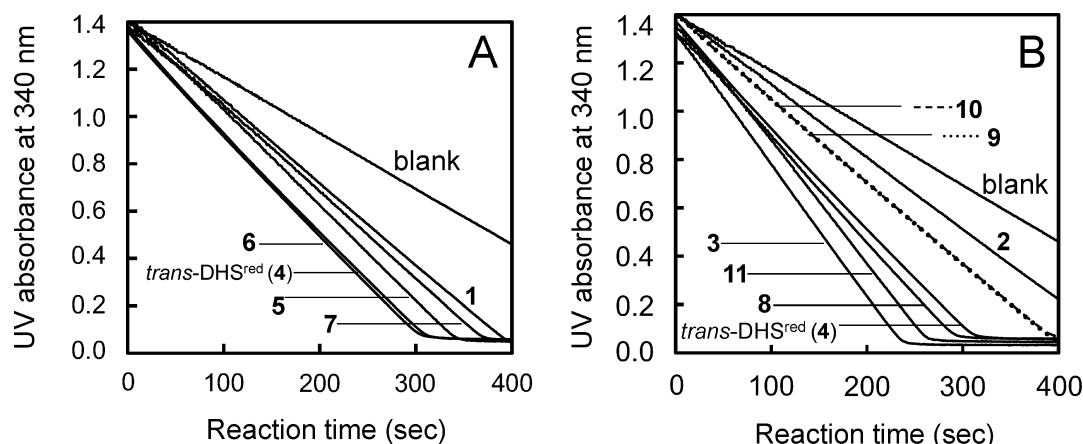


Figure 2. NADPH-coupled GPx assay for water-soluble selenides (A) 1 and 4–7 and (B) 2–4 and 8–10. Reaction conditions were $[\text{GSH}]_0 = 1.0$ mM, $[\text{H}_2\text{O}_2]_0 = 2.5$ mM, $[\text{NADPH}]_0 = 0.3$ mM, $[\text{GR}] = 4$ units/mL, and $[\text{selenide}] = 0.2$ mM in pH 7.4 phosphate buffer at 25 °C. The results for selenides 1–4 are quoted from ref 21.

Table 2. Summary of GPx-Like Catalytic Activities of Selenides in Water and in MeOH, along with Second-Order Rate Constants for Oxidation and HOMO Energy Levels

selenide	ν_0^a ($\mu\text{M min}^{-1}$)	t_{50}^b (min)	k_{ox}^c ($\text{M}^{-1} \text{s}^{-1}$)	HOMO in vacuo ^d (eV)	substituent(s)	HOMO in water ^e (eV)	substituent(s)
no catalyst	32.2 (± 3.2)	>300	–	–			
1	44.2 (± 2.4)	90	0.26 (± 0.02)	–6.07	OH	–6.20	OH
2	34.5 (± 1.1)	10	0.06 (± 0.01)	–5.83	NH_2	–6.69	NH_3^+
3	71.1 (± 6.9)	100	0.87 (± 0.02)	–6.10	CO_2H	–5.72	CO_2^-
<i>trans</i> -DHS ^{red} (4)	54.2 (± 4.0)	40	0.57 (± 0.03) ^f	–6.12	OH_{ax} , OH_{ax}	–6.16	OH_{ax} , OH_{ax}
5	50.7 (± 2.5)	95	ND ^g	–5.90	OH_{eq}	–6.06	OH_{eq}
<i>cis</i> -DHS ^{red} (6)	54.3 (± 3.7)	15	ND ^g	–5.86	OH_{eq} , OH_{ax}	–6.01	OH_{eq} , OH_{ax}
7	45.7 (± 1.5)	275	ND ^g	–6.20	OH_{eq} , OH_{eq} , OH_{eq}	–6.21	OH_{eq} , OH_{eq} , OH_{eq}
MAS ^{red} (8)	59.8 (± 1.1)	20	0.47 (± 0.05)	–5.50	$\text{NH}_{2\text{ax}}$	–6.44	NH_3^+ _{ax}
<i>trans</i> -DAS ^{red} (9)	47.2 (± 4.3)	6	0.14 (± 0.02)	–5.32	$\text{NH}_{2\text{ax}}$, $\text{NH}_{2\text{ax}}$	–6.87	NH_3^+ _{ax} , NH_3^+ _{ax}
<i>cis</i> -DAS ^{red} (10)	48.2 (± 5.3)	65	0.13 (± 0.02)	–5.52	$\text{NH}_{2\text{eq}}$, $\text{NH}_{2\text{ax}}$	–6.88	NH_3^+ _{eq} , NH_3^+ _{ax}
11	63.8 (± 1.0)	120	ND ^g	–6.02	$\text{CO}_2\text{H}_{\text{eq}}$	–5.74	CO_2^- _{eq}

^aInitial rates (ν_0) of H_2O_2 reduction in phosphate buffer at pH 7.4 and 25 °C. Values calculated from the slope of the UV absorbance changes in the range of 0–60 s in Figure 2A,B. ^bReaction times for 50% conversion of DTT^{red} to DTT^{ox} in MeOH. See Figure 3 for reaction conditions. ^cSecond-order rate constants for the oxidation of selenides with H_2O_2 in water at 25 °C (i.e., reaction A in Scheme 1). ^dHOMO energy levels calculated at the B3LYP/6-31+G(d,p) level in vacuo. ^eHOMO energy levels calculated at the B3LYP/6-31+G(d,p) level in water using the polarizable continuum model (PCM). ^fData quoted from ref 21. ^gNot determined.

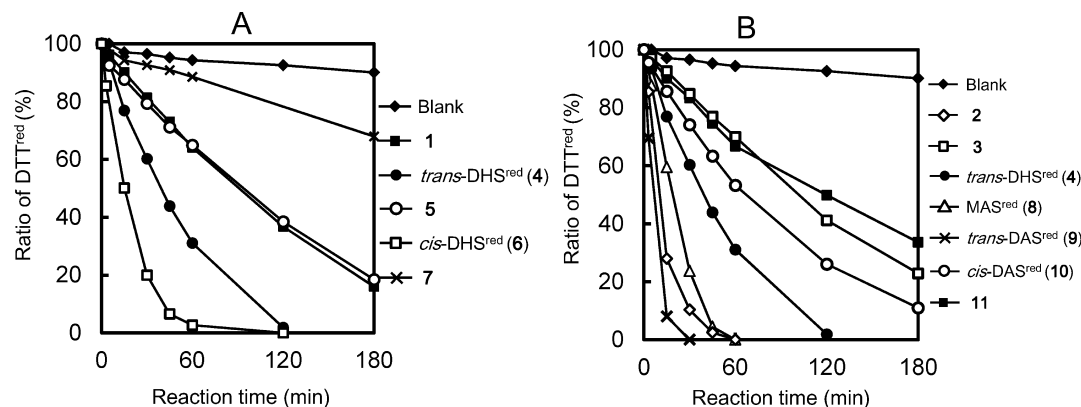


Figure 3. Percentages of residual DTT^{red} as a function of reaction time in the oxidation of DTT^{red} with H_2O_2 in the presence of a selenide catalyst (1–11) in CD_3OD . The selenide catalyst was (A) 1, 4, 5, 6, or 7; (B) 2, 3, 4, 8, 9, 10, or 11. Reaction conditions were $[\text{DTT}^{\text{red}}]_0 = [\text{H}_2\text{O}_2]_0 = 0.14$ mM and $[\text{selenide}] = 0.014$ mM at 25 °C.

20%. These results indicate that the reducing ability of a five-membered ring selenide is higher than that of a four-membered

ring selenide. This finding is consistent with the order of GPx-like activities observed for 4 and 5 in water (Figure 2).

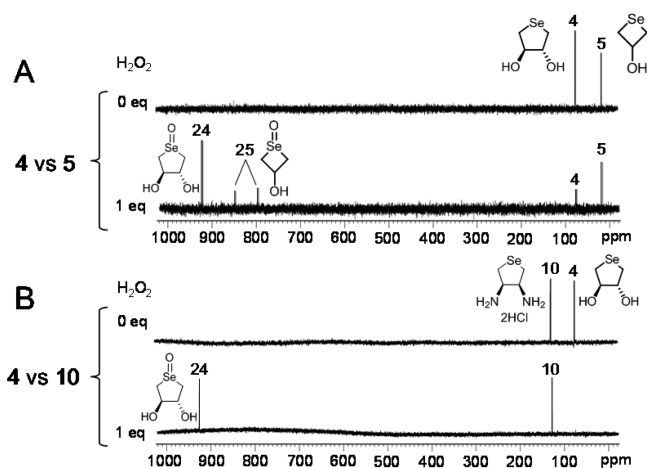


Figure 4. ^{77}Se NMR spectral changes observed for the competitive oxidation of (A) selenides 4 and 5 (0.025 mmol each) and (B) selenides 4 and 10 (0.025 mmol each) with H_2O_2 (0.025 mmol) in D_2O (0.7 mL) at 25 °C.

Similarly, when the oxidations of selenides 4 and 10 with H_2O_2 in D_2O were compared (Figure 4B), 4 was more readily oxidized than 10. The result is again consistent with the order of the GPx-like activity in water (Figure 2). A similar result was obtained in a competitive experiment using selenides 4 and 9. According to the results obtained from the competitive experiments for various combinations of the selenides, the order of the reducing ability was eventually determined to be $3 \approx 11 > 4 \approx 6 \approx 8 > 1 \approx 5 \approx 7 \geq 9 \approx 10 > 2$. This order is consonant with the order of the GPx-like activities in aqueous medium (Figure 2 and Table 2), strongly supporting the conclusion that the rate-determining step in the GPx-like catalytic cycle of selenides is the oxidation process.

The same examination was performed in CD_3OD as the solvent to obtain information on the relationship between the ease of the oxidation step (reaction A in Scheme 1) and the GPx-like activity in methanol (Figure 3). Surprisingly, the order of reducing ability of the selenides in methanol was completely identical to that determined in water (i.e., $3 \approx 11 > 4 \approx 6 \approx 8 > 1 \approx 5 \approx 7 \geq 9 \approx 10 > 2$) and did not have any correlation with the order of the GPx-like activity in methanol (i.e., $9 \approx 10 > 2 > 8 > 4 > 6 > 5 \approx 1 > 3 > 11 > 7$). This can be explained by switching the rate-determining step of the catalytic cycle in methanol from reaction A to B. However, it was confirmed that the reaction rate for reaction A (~ 1 h) is obviously lower than that for reaction B (< 5 min) when the conversion between *trans*-DHS^{red} (4) and *trans*-DHS^{ox} (24) was monitored by ^1H NMR spectroscopy. Although the oxidation rate in methanol was greater than that in water (~ 2 h), the rate-determining step in methanol was still reaction A. Another possible reason for the observed discrepancy between the reducing abilities of the selenides and the GPx-like activities in methanol might be that the reaction progresses through a different cycle from that shown in Scheme 1. Recently, Nascimento et al. reported that the oxidation of PhSH with H_2O_2 in methanol catalyzed by an aryl benzyl selenide/selenoxide redox system can proceed through a hydroxy perhydroxy selenane intermediate formed by further oxidation of the selenoxide with H_2O_2 .²⁴ Back et al. reported formation of a spiro selenium species for similar open-chain selenides.²³ Participation of such highly reactive species could explain the observed discrepancy, but such species were not observed in our NMR analysis. At this moment, there is no

effective scenario to explain the order of GPx-like activities observed for selenides 1–11 in methanol.

Second-Order Rate Constants for Reaction A. To further investigate the relationship between the reducing abilities of the selenides and the GPx-like antioxidant activities in aqueous medium, the second-order rate constants (k_{ox}) for the oxidation of the selenides with H_2O_2 to the corresponding selenoxides (i.e., reaction A in Scheme 1) were estimated as follows. It is known that the UV spectrum of a selenide changes during the conversion to the selenoxide.²¹ Indeed, the selenides employed in this study exhibited clear UV spectral changes with the progress of the oxidation to the selenoxides. A representative example is shown in Figure 5 for the case of the oxidation of 9

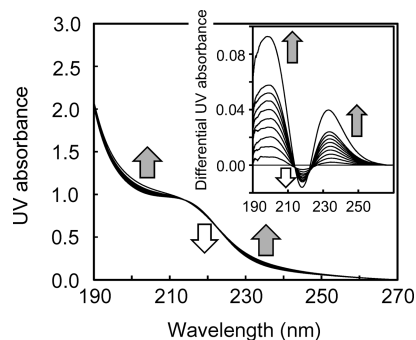


Figure 5. (A) UV spectral changes and (B) differential UV spectra observed in the oxidation of selenide 9 with H_2O_2 . Reaction conditions were $[9]_0 = 0.3$ mM and $[\text{H}_2\text{O}_2]_0 = 2$ mM in water at 25 °C. Reaction time was 0–50 min.

to 20. The reaction rate was then determined by analyzing the time course of the absorbance change at 234 nm. The second-order rate constants (k_{ox}) for the oxidations of 1–4 and 8–10 to the corresponding selenoxides 21–24, 28, 20, and 29, respectively, were determined by plotting the observed pseudo-first-order rate constants (k_{obs}) against the concentration of H_2O_2 (Figure 6). The values of k_{ox} estimated from the slopes

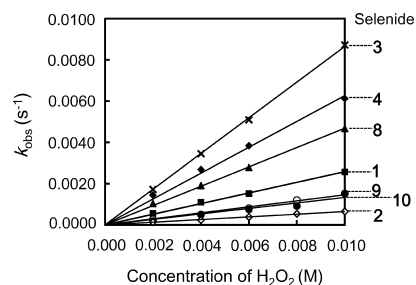


Figure 6. Linear plots showing the dependence of the observed pseudo-first-order rate constants (k_{obs}) for the oxidations of selenides 1–4 and 8–10 (0.3 mM) with H_2O_2 .

are summarized in the fourth column of Table 2. The magnitude decreases in the order, $3 > 4 > 8 > 1 > 9 \approx 10 > 2$, which well matches the order of the GPx-like activity in aqueous medium (i.e., $3 > 8 > 4 > 1 \approx 9 \approx 10 > 2$) except for the order of 4 and 8. The correlation plots, namely, v_0 vs k_{ox} are shown in Figure 7. The positive correlation confirms that the reducing ability of a selenide can control the GPx-like activity in an aqueous medium.

HOMO Energy Levels. The HOMO energy levels of selenides 1–11 were obtained by quantum chemical calcu-

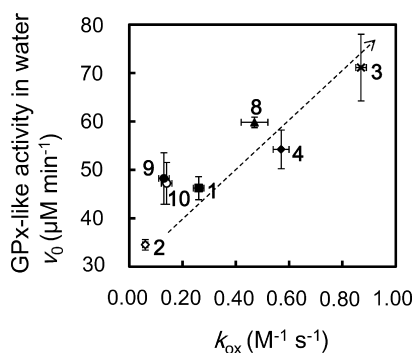


Figure 7. Correlation plot of the GPx-like activity (v_0) of selenides 1–4 and 8–10 in water vs the second-order rate constants (k_{ox}) for the oxidations of the selenides to the corresponding selenoxides.

lations at the B3LYP/6-31+G(d,p) level in vacuo and also in water applying the polarizable continuum model (PCM). The results are reported on the right side of Table 2. For all selenides, the HOMO is dominantly localized at the selenium atom, indicating that the oxidation rate of the selenides to the selenoxides should be controlled by the HOMO energy level.

Plots of the GPx-like activities observed for selenides 1–11 in methanol (i.e., the reaction times for 50% conversion of DTT^{red}, t_{50}) against the HOMO energy levels in vacuo failed to give a clear correlation curve (Figure 8). Thus, the GPx-like

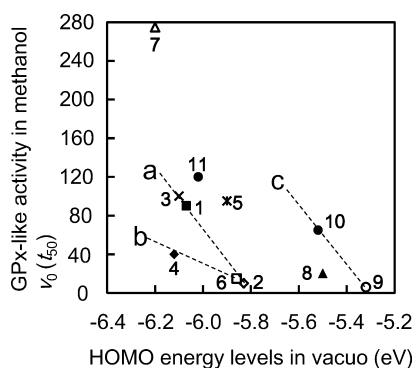


Figure 8. Correlation plots between the HOMO energy levels of selenides 1–11 in vacuo and the GPx-like activities in methanol (t_{50}).

activity in methanol should not be determined simply by the feasibility of the selenides to reduce H_2O_2 . Nevertheless, there seems to be a weak tendency that a higher HOMO results in a shorter t_{50} if one focuses on some series of selenides. For example, the activity of open-chain selenides 1–3 increases with elevation of the HOMO level (dashed line a). Similar correlations seem to exist for the DHS (4 and 6) and DAS (9 and 10) series (dashed lines b and c, respectively).

On the other hand, a clear correlation was obtained in water between the HOMO energy level and the GPx-like activity (v_0), as shown in Figure 9. The correlation supports the conclusion that the GPx-like antioxidant activity in water is controlled by the reducing ability of the selenide. For the selenides with NH_2 group(s), namely, MAS^{red} (8), *trans*-DAS^{red} (9), and *cis*-DAS^{red} (10), however, the plots obviously deviate from the correlation line. This can be explained by considering an equilibrium between the ionized and neutral forms in water. If such an equilibrium exists, the HOMO would be elevated, and the plots should move toward the correlation line.

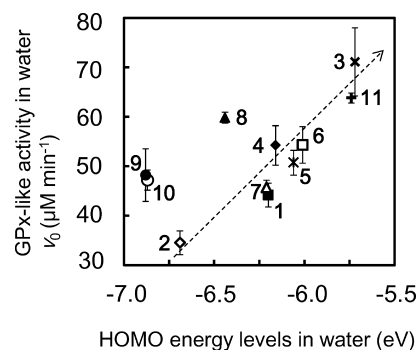


Figure 9. Correlation plots between the HOMO energy levels of selenides 1–11 in water and the GPx-like activities in a phosphate buffer solution (v_0).

CONCLUSIONS

In this work, we synthesized the series of water-soluble cyclic selenides 5–11 and compared their GPx-like antioxidant activities to reference selenides 1–4. As a result, several clues were obtained for the molecular design of cyclic selenides with enhanced GPx-like activities. (1) The optimal ring size is five. (2) Substituents can control the activity. In general, the activity increases by changing the substituent from NH_2 to OH and then CO_2H in water, but this order is inverted in methanol. (3) The number of substituents also controls the activity, but this effect does not always hold [e.g., MAS^{red} (8) showed higher activity than DAS^{red} (9 and 10) in water]. (4) The stereoconfiguration of the substituents does not affect the activity in water, but it has a strong impact in methanol. (5) Regarding solvent effects, the activity is enhanced in methanol, but the rank of the activity in methanol cannot be explained by simple scenarios based on the reducing ability of the selenides and the HOMO energy levels. Although more extensive study is necessary to fully understand the observed GPx-like activities, especially in methanol, these findings will be useful in a future study for development of small molecular GPx mimics or antioxidant selenium drugs.

EXPERIMENTAL SECTION

General. 1H (500 MHz), ^{13}C (125.8 MHz), and ^{77}Se (95.4 MHz) NMR spectra were recorded at 298 K, and coupling constants (J) are reported in hertz. High-resolution mass spectra were recorded under atmospheric pressure chemical ionization (APCI+) or electrospray ionization (ESI+) conditions. All reactions for the synthesis of selenides were monitored by thin-layer chromatography (TLC). Gel permeation chromatography (GPC) was performed with a general isocratic HPLC system using $CHCl_3$ as the eluent. Ultraviolet (UV) spectra were measured at 25.0 °C using a circulating water-bath system. Selenides 1,²⁰ 2,²⁰ 3,²⁰ 4,²⁷ 5,²⁸ 7,^{29,30} 8,³¹ and 11²⁰ were prepared as described. Compounds 12,³² 17a,³⁶ and 17b^{37–39} were prepared by following previous literature procedures. All other chemicals were used as purchased without further purification.

(cis-2,2-Dimethyl-1,3-dioxolane-4,5-diyl)dimethanol (14).³⁴ Diol 12 (990 mg, 3.3 mmol) was mixed with 2,2-dimethoxypropane (DMP) (13.5 mL) and *p*-toluenesulfonic acid (*p*-TsOH) (52 mg, 0.30 mmol). After the mixture had been stirred for 2 h at 35 °C, the solution was neutralized with a saturated aqueous $NaHCO_3$ solution (40 mL) and further stirred for 1 h. The resulting solution was extracted with EtOAc (30 mL × 1). The organic layer was washed with brine (40 mL × 1), dried over $MgSO_4$, and concentrated under a vacuum to give 13 as a slightly yellow oil. Yield: 1.12 g (96%). 1H NMR (500 MHz, $CDCl_3$): δ 7.17 (m, 10H), 4.39 (q, $J = 18.3$, 4H), 4.23 (m, 2H), 3.43 (m, 4H), 1.34 (s, 3H), 1.26 (s, 3H). The 1H NMR

spectroscopic data of **13** are in good agreement with those reported in the literature.³³

Then, **13** (2.97 g, 8.67 mmol) was dissolved in MeOH (18 mL) and vigorously stirred for 24 h at room temperature in the presence of Pd/C as a catalyst under a hydrogen atmosphere. The resulting solution was filtered to remove Pd/C and concentrated in vacuo to give **14** as a colorless oil. Yield: 1.26 g (90%). ¹H NMR (500 MHz, CD₃OD): δ 4.25 (m, 2H), 3.67 (m, 4H), 1.44 (s, 3H), 1.36 (s, 3H). ¹³C NMR (125.8 MHz, CD₃OD): δ 108.1, 77.4, 60.2, 26.8, 24.1.

(*cis*-2,2-Dimethyl-1,3-dioxolane-4,5-diyl)bis(methylene) Dime-thanesulfonate (**15**).³⁴ To a cooled (0 °C) solution of **14** (0.60 g, 3.68 mmol) in pyridine (3 mL) was slowly added methanesulfonyl chloride (MsCl) (855 μL, 11.0 mmol). After the mixture solution had been stirred for 2.5 h at room temperature, 50 mM HCl (20 mL) was added, and the solution was further stirred for 10 min. The resulting solution was extracted with EtOAc (25 mL × 3), and then the organic layer was washed with water (20 mL × 1) and brine (20 mL × 1), dried over MgSO₄, and concentrated in vacuo. The obtained residual material was purified by silica gel column chromatography (EtOAc/*n*-hexane 1:1) to give **15** as a white solid. Yield: 0.76 g (65%). R_f: 0.29 (EtOAc/*n*-hexane 1:1). ¹H NMR (500 MHz, CDCl₃): δ 4.51 (m, 2H), 4.37 (m, 4H), 3.11 (s, 6H), 1.51 (s, 3H), 1.41 (s, 3H). ¹³C NMR (125.8 MHz, CDCl₃): δ 110.2, 74.2, 66.4, 37.7, 27.5, 25.1.

cis-3,4-Dihydroxytetrahydrosele-nophene (*cis*-DHS^{red}) (**6**).³⁵ Selenium powder (0.18 g, 2.28 mmol) and sodium borohydride (0.26 g, 6.87 mmol) were placed in a two-necked round-bottomed flask. After replacement of the air in the flask with nitrogen gas, anhydrous EtOH (11 mL) was added. The mixture was stirred and heated under reflux conditions for 45 min to generate sodium hydrogen selenide (NaHSe) in situ. A solution of **15** (0.37 g, 1.16 mmol) in anhydrous THF (7 mL) was added to the resulting colorless solution through a glass syringe. After being heated under reflux conditions for 2.5 h, the mixture was cooled to room temperature and extracted with EtOAc (25 mL × 3). The organic layer was washed with brine (40 mL × 1), dried over MgSO₄, and concentrated in vacuo. The residual yellow solid was purified by silica gel column chromatography (EtOAc/*n*-hexane 1:2) and then by GPC to give **6** as a white solid. Yield: 160 mg (65%). mp: 52.9–54.5 °C. R_f: 0.61 (EtOAc/*n*-hexane 1:2). ¹H NMR (500 MHz, CDCl₃): δ 4.84 (m, 2H), 2.94 (m, 4H), 1.46 (s, 3H), 1.26 (s, 3H). ¹³C NMR (125.8 MHz, CDCl₃): δ 110.4, 84.5, 30.3, 26.4, 24.41. ⁷⁷Se NMR (95.4 MHz, CDCl₃): δ 162.8.

Then, an aqueous AcOH (4.5 mL, 80%) was added to a solution of **6** (0.16 g, 7.69 mmol) in MeOH (4.5 mL). The mixture was vigorously stirred under reflux conditions for 16.5 h. The resulting solution was evaporated to remove residual MeOH and azeotropically dried with EtOAc (20 mL) to give **6** as a white solid. Yield: 0.13 g (quantitative). mp: 78–80 °C. R_f: 0.51 (Et₂O/EtOAc 1:1). ¹H NMR (500 MHz, D₂O): δ 4.22 (m, 2H), 2.93 (m, 2H), 2.65 (m, 2H). ¹³C NMR (125.8 MHz, D₂O): δ 76.1, 23.3. ⁷⁷Se NMR (95.4 MHz, D₂O): δ 83.6.

threo-2,3-Bis(*tert*-butoxycarbonylamino)butane-1,4-diyl Dime-thanesulfonate (**18a**). MsCl (100 μL, 1.27 mmol) was slowly added to a cooled (0 °C) solution of **17a** (177 mg, 0.55 mmol) in pyridine (5 mL). After being stirred at 0 °C for 3.5 h, the resulting solution was poured into chilled water (1 °C). Precipitates were filtered under diminished pressure and dried overnight in the atmosphere to give **18a** as a white solid material. Yield: 230 mg (88%). mp: 103–107 °C. R_f: 0.65 (EtOAc/hexane 1:2). ¹H NMR (500 MHz, CDCl₃): δ 5.19 (d, *J* = 7.0, 2H), 4.26 (m, 4H), 4.02 (m, 2H), 3.00 (s, 6H), 1.38 (s, 18H). ¹³C NMR (125.8 MHz, CDCl₃): δ 155.9, 80.7, 68.1, 50.4, 37.5, 28.3. HRMS (APCI-TOF) *m/z*: [M + Na]⁺ calcd for C₁₆H₃₂N₂O₁₀S₂Na, 499.1396; found, 499.1423.

erythro-2,3-Bis(*tert*-butoxycarbonylamino)butane-1,4-diyl Dime-thanesulfonate (**18b**). Compound **18b** was synthesized from **17b** (574 mg, 1.79 mmol) by a procedure similar to that used for the synthesis of **18a**. It was obtained as a white solid material. Yield: 775 mg (91%). mp: 169–171 °C. R_f: 0.77 (EtOAc/hexane 1:2). ¹H NMR (500 MHz, *d*-DMSO): δ 4.16 (m, 4H), 3.85 (s, 2H), 3.35 (s, 2H), 3.14 (s, 6H), 1.40 (s, 18H). ¹³C NMR (125.8 MHz, *d*-DMSO): δ

155.7, 79.0, 69.4, 49.8, 37.1, 28.6. HRMS (APCI-TOF) *m/z*: [M + Na]⁺ calcd for C₁₆H₃₂N₂O₁₀S₂Na, 499.1396; found, 499.1423.

trans-3,4-Bis(*tert*-butyloxycarbonylamino) Tetrahydrosele-nophene (**19a**). Selenium powder (103 mg, 1.12 mmol) and sodium borohydride (184 mg, 4.86 mmol) were placed in a two-necked round-bottomed flask. After replacement of the air in the flask with nitrogen gas, anhydrous EtOH (8 mL) was added. The mixture was stirred and heated under reflux conditions for 30 min under a nitrogen atmosphere to generate sodium hydrogen selenide (NaHSe) in situ. A solution of **18a** (190 mg, 0.40 mmol) in anhydrous THF (12 mL) was added to the resulting colorless solution at 45 °C through a glass syringe. After the mixture had been heated under reflux conditions for 4 h, water (40 mL) was added, and extraction was conducted with CH₂Cl₂ (50 mL × 3). The combined organic layers were washed with brine (40 mL × 1), dried over MgSO₄, and concentrated under a vacuum. The residual yellow solid was purified by silica gel column chromatography (Et₂O/*n*-hexane 2:1) and then by GPC to give **19a** as a white solid. Yield: 118 mg (81%). mp: 193–194 °C. R_f: 0.33 (Et₂O/*n*-hexane 2:1). ¹H NMR (500 MHz, CDCl₃): δ 4.87 (s, 2H), 4.11 (s, 2H), 3.08 (m, 2H), 2.67 (m, 2H), 1.43 (s, 18H). ¹³C NMR (125.8 MHz, CDCl₃): δ 155.6, 79.9, 59.0, 28.3, 23.4. ⁷⁷Se NMR (95.4 MHz, CDCl₃): δ 87.6. HRMS (APCI-TOF) *m/z*: [M + Na]⁺ calcd for C₁₄H₂₆N₂O₄SeNa, 389.0956; found, 389.0977.

cis-3,4-Bis(*tert*-butyloxycarbonylamino) Tetrahydrosele-nophene (**19b**). Compound **19b** was synthesized from **18b** (206 mg, 0.43 mmol) by a procedure similar to that used for the synthesis of **19a**. It was obtained as a white solid. Yield: 131 mg (83%). mp: 136–138 °C. R_f: 0.29 (Et₂O/*n*-hexane 2:1). ¹H NMR (500 MHz, CDCl₃): δ 5.16 (d, *J* = 5.9, 2H), 4.27 (m, 2H), 3.17 (m, 2H), 2.56 (m, 2H), 1.42 (s, 18H). ¹³C NMR (125.8 MHz, CDCl₃): δ 155.7, 79.9, 57.4, 28.3, 24.2. ⁷⁷Se NMR (95.4 MHz, CDCl₃): δ 104.5, 100.8. HRMS (APCI-TOF) *m/z*: [M + Na]⁺ calcd for C₁₄H₂₆N₂O₄SeNa, 389.0956; found, 389.0977.

trans-3,4-Diaminetetrahydrosele-nophene-2HCl (*trans*-DAS^{red}) (**9**). HCl (2 mL, 4 M) was added to a solution of **19a** (33.0 mg, 0.09 mmol) in THF (2 mL). The mixture was vigorously stirred for 18 h at room temperature. After removal of the ethereal layer by evaporation, the aqueous solution was diluted with water (30 mL) and lyophilized to give **9** as a white powder. Yield: 22.6 mg (quantitative). mp: 199 °C (decomp). ¹H NMR (500 MHz, D₂O): δ 4.25 (m, 2H), 3.27 (m, 2H), 3.11 (m, 2H). ¹³C NMR (125.8 MHz, D₂O): δ 57.6, 22.7. ⁷⁷Se NMR (95.4 MHz, D₂O): δ 121.5. HRMS (APCI-TOF) *m/z*: [M + H – 2HCl]⁺ calcd for C₄H₁₁N₂Se, 167.0082; found, 167.0043.

cis-3,4-Diaminetetrahydrosele-nophene-2HCl (*cis*-DAS^{red}) (**10**). Compound **10** was synthesized from **19b** (22.1 mg, 0.06 mmol) by a procedure similar to that used for the synthesis of **9**. It was obtained as a white powder. Yield: 14.1 mg (quantitative). mp: 173 °C (decomp). ¹H NMR (500 MHz, D₂O): δ 4.21 (m, 2H), 3.30 (m, 2H), 2.90 (m, 2H). ¹³C NMR (125.8 MHz, D₂O): δ 57.6, 30.3. ⁷⁷Se NMR (95.4 MHz, D₂O): δ 121.5. HRMS (APCI-TOF) *m/z*: [M + H – 2HCl]⁺ calcd for C₄H₁₁N₂Se, 167.0082; found, 167.0043.

NADPH-Coupled GPx Activity Assay Using GSH as a Thiol Substrate.⁴⁰ A test solution was prepared by mixing a 100 mM phosphate/6 mM EDTA buffer solution (1941 μL) at pH 7.4 containing NADPH (2.0 μmol) and GSH (6.8 μmol) with a GR solution (453 U/mL, 59 μL). An aliquot (300 μL) of the test solution was added to a 1.0 mM selenide solution (200 μL) in 100 mM phosphate buffer at pH 7.4, and the resulting solution was diluted with the phosphate buffer solution (430 μL) and maintained at 25 °C. The reaction was initiated by addition of a 36 mM aqueous H₂O₂ solution (70 μL) to the mixture solution. The reaction progress was monitored by the absorption changes at 340 nm due to consumption of NADPH. The initial concentrations of selenide, H₂O₂, GSH, NADPH, and GR in the assay solution were 0.2 mM, 2.5 mM, 1.0 mM, 0.3 mM, and 4 U/mL, respectively.

GPx Activity Assay Using DTT^{red} as a Dithiol Substrate. The activity assay was performed following the literature method.²⁰ DTT^{red} (0.15 mmol) and selenide (0.015 mmol) were dissolved in CD₃OD (1.1 mL), and the solution was mixed with 30% H₂O₂ (17 μL, 0.15 mmol) to start the reaction. ¹H NMR spectra were measured at

variable reaction times at 25 °C. The relative populations of DTT^{red} and DTT^{ox} were determined by integration of the ¹H NMR absorptions, which were well-isolated in the spectrum.

Kinetic Analysis. The rate constant (k_{obs}) of the reaction between H₂O₂ (2.0–10.0 mM) and selenide (0.3 mM) was measured at 25 °C in water by following the UV absorption change at 225, 228, 221, 225, 222, 234, or 236 nm for selenides 1–4 and 8–10, respectively. The measurement was repeated more than three times. The obtained k_{obs} values were then plotted against the concentration of H₂O₂ to determine the second-order rate constants (k_{ox}) for reaction A in Scheme 1.

Quantum Chemical Calculation. The Gaussian 09 software package (revision B.01)⁴¹ was employed. The structures were optimized in vacuo and in water at the B3LYP/6-31+G(d,p) level. The polarizable continuum model (PCM)^{42–45} was applied for the calculation in water. For the linear selenides (1–3), an extended conformation with all dihedral angles anti was employed as the initial structure. For the cyclic selenides (4–11), all possible stereo-configurations were tested, and the obtained global-minimum-energy structure was used for the analysis of experimental data. Frequency calculations were performed for the obtained minimum-energy structures to confirm that the structures had no imaginary frequencies. The structures thus obtained were used for analyzing the energy levels and the shapes of the molecular orbitals.

■ ASSOCIATED CONTENT

● Supporting Information

¹H and ¹³C NMR spectra of compounds 6, 9, 10, 13–16, 18a, 18b, 19a, and 19b; ¹H NMR spectral changes in the redox reactions of selenide 9 and selenoxide 20; and structures optimized by quantum chemical calculations. The Supporting Information is available free of charge on the ACS Publications website at DOI: 10.1021/acs.joc.5b00544.

■ AUTHOR INFORMATION

Corresponding Author

*E-mail: miwaoka@tokai.ac.jp.

Notes

The authors declare no competing financial interest.

■ ACKNOWLEDGMENTS

This work was supported financially by the Ministry of Education, Culture, Sports, Science and Technology of Japan [Grant-in-Aid for Scientific Research (C) 23550198]. We gratefully acknowledge Mr. Takuro Sato (Tokai University) for technical support.

■ REFERENCES

- Böck, A.; Forchhammer, K.; Heider, J.; Leinfelder, W.; Sawers, G.; Veprek, B.; Zinoni, F. *Mol. Microbiol.* **1991**, *5*, 515–520.
- Flohé, L.; Günzler, W. A.; Schock, H. H. *FEBS Lett.* **1973**, *32*, 132–134.
- Savaskan, N. E.; Ufer, C.; Kühn, H.; Borchert, A. *Biol. Chem.* **2007**, *5*, 1007–1017.
- Conrad, M.; Schneider, M.; Seiler, A.; Bornkamm, G. W. *Biol. Chem.* **2007**, *388*, 1019–1025.
- Toppo, S.; Flohé, L.; Ursini, F.; Vanin, S.; Maiorino, M. *Biochim. Biophys. Acta, Gen. Subj.* **2009**, *1790*, 1486–1500.
- Bhabak, K. P.; Mughesh, G. *Acc. Chem. Res.* **2010**, *43*, 1408–1419.
- Alberto, E. E.; do Nascimento, V.; Braga, A. L. *J. Braz. Chem. Soc.* **2010**, *21*, 2032–2041.
- Huang, X.; Liu, X.; Luo, Q.; Liu, J.; Shen, J. *Chem. Soc. Rev.* **2011**, *40*, 1171–1184.
- Santi, C.; Tidei, C.; Scalera, C.; Piroddi, M.; Galli, F. *Curr. Chem. Biol.* **2013**, *7*, 25–36.
- Mughesh, G. *Curr. Chem. Biol.* **2013**, *7*, 47–56.

(11) Iwaoka, M. Antioxidant organoselenium molecules. In *Organoselenium Chemistry between Synthesis and Biochemistry*; Santi, C., Ed.; Bentham Science Publishers: Sharjah, United Arab Emirates, 2014; Chapter 12, pp 361–378.

(12) Wilson, S. R.; Zucker, P. A.; Huang, R. R. C.; Spector, A. *J. Am. Chem. Soc.* **1989**, *111*, 5936–5939.

(13) Iwaoka, M.; Tomoda, S. *J. Am. Chem. Soc.* **1994**, *116*, 2557–2561.

(14) Bhabak, K. P.; Mughesh, G. *Chem.—Eur. J.* **2008**, *14*, 8640–8651.

(15) Mughesh, G.; Panda, A.; Singh, H. B.; Butcher, R. J. *Chem.—Eur. J.* **1999**, *5*, 1411–1421.

(16) Wirth, T. *Molecules* **1998**, *3*, 164–166.

(17) Collins, C. A.; Fry, F. H.; Holme, A. L.; Yiakouvakaki, A.; Al-Qenaie, A.; Pourzand, C.; Jacob, C. *Org. Biomol. Chem.* **2005**, *3*, 1541–1546.

(18) Prabhu, C. P.; Phadnis, P. P.; Wadawale, A. P.; Priyadarsini, K. I.; Jain, V. K. *J. Organomet. Chem.* **2012**, *713*, 42–50.

(19) Nascimento, V.; Ferreira, N. L.; Canto, R. F. S.; Schott, K. L.; Waczuk, E. P.; Sancineto, L.; Santi, C.; Rocha, J. B. T.; Braga, A. L. *Eur. J. Med. Chem.* **2014**, *87*, 131–139.

(20) Iwaoka, M.; Kumakura, F. *Phosphorus Sulfur Silicon Relat. Elem.* **2008**, *183*, 1009–1017.

(21) Kumakura, F.; Mishra, B.; Priyadarsini, K. I.; Iwaoka, M. *Eur. J. Org. Chem.* **2010**, 440–445.

(22) Rahmanto, A. S.; Davies, M. J. *Free Radical Biol. Med.* **2011**, *51*, 2288–2299.

(23) Back, T. G.; Moussa, Z.; Parvez, M. *Angew. Chem., Int. Ed.* **2004**, *43*, 1268–1270.

(24) Nascimento, V.; Alberto, E. E.; Tondo, D. W.; Dambrowski, D.; Detty, M. R.; Nome, F.; Braga, A. L. *J. Am. Chem. Soc.* **2012**, *134*, 138–141.

(25) Prabhu, P.; Bag, P. P.; Singh, B. G.; Hodage, A.; Jain, V. K.; Iwaoka, M.; Priyadarsini, K. I. *Free Radical Res.* **2011**, *45*, 461–468.

(26) Arai, K.; Dedachi, K.; Iwaoka, M. *Chem.—Eur. J.* **2011**, *17*, 481–485.

(27) Iwaoka, M.; Takahashi, T.; Tomoda, S. *Heteroatom Chem.* **2001**, *12*, 293–299.

(28) Polson, G.; Dittmer, D. C. *J. Org. Chem.* **1988**, *53*, 791–794.

(29) Crombez-Robert, C.; Benazza, M.; Fréchou, C.; Demailly, G. *Carbohydr. Res.* **1997**, *303*, 359–365.

(30) Szczepina, M. G.; Johnston, B. D.; Yuan, Y.; Svensson, B.; Pinto, B. M. *J. Am. Chem. Soc.* **2004**, *126*, 12458–12469.

(31) Arai, K.; Moriai, K.; Ogawa, A.; Iwaoka, M. *Chem.—Asian J.* **2014**, *9*, 3464–3471.

(32) Nishizono, N.; Akama, Y.; Agata, M.; Sugo, M.; Yamaguchi, Y.; Oda, K. *Tetrahedron* **2011**, *67*, 358–363.

(33) Balamurugan, R.; Kothapalli, R. B.; Thota, G. K. *Eur. J. Org. Chem.* **2011**, 1557–1569.

(34) Nishizono, N.; Babe, R.; Nakamura, C.; Oda, K.; Machida, M. *Org. Biomol. Chem.* **2003**, *1*, 3692–3697.

(35) Nakayama, J.; Shibuya, M.; Ikuina, Y.; Murai, F.; Hoshino, M. *Phosphorus Sulfur Silicon Relat. Elem.* **1988**, *38*, 149–155.

(36) Martin, R. L.; Norcross, B. E. *J. Org. Chem.* **1975**, *40*, 523–524.

(37) Wu, F.-L.; Ross, B. P.; McGeary, R. P. *Eur. J. Org. Chem.* **2010**, 1989–1998.

(38) Scheurer, A.; Mosset, P.; Saalfrank, R. W. *Tetrahedron: Asymmetry* **1997**, *8*, 1243–1251.

(39) Lee, S. H.; Kohn, H. *J. Am. Chem. Soc.* **2004**, *126*, 4281–4292.

(40) Pascual, P.; Martínez-Lara, E.; Bárcena, J. A.; López-Barea, J.; Toribio, F. *J. Chromatogr. B: Biomed. Sci. Appl.* **1992**, *581*, 49–56.

(41) Frisch, M. J.; Trucks, G. W.; Schlegel, H. B.; Scuseria, G. E.; Robb, M. A.; Cheeseman, J. R.; Scalmani, G.; Barone, V.; Mennucci, B.; Petersson, G. A.; Nakatsuji, H.; Caricato, M.; Li, X.; Hratchian, H. P.; Izmaylov, A. F.; Bloino, J.; Zheng, G.; Sonnenberg, J. L.; Hada, M.; Ehara, M.; Toyota, K.; Fukuda, R.; Hasegawa, J.; Ishida, M.; Nakajima, T.; Honda, Y.; Kitao, O.; Nakai, H.; Vreven, T.; Montgomery, J. A., Jr.; Peralta, J. E.; Ogliaro, F.; Bearpark, M.; Heyd, J. J.; Brothers, E.; Kudin, K. N.; Staroverov, V. N.; Keith, T.; Kobayashi, R.; Normand, J.; Raghavachari, K.; Rendell, A.; Burant, J. C.; Iyengar, S. S.; Tomasi, J.;

Cossi, M.; Rega, N.; Millam, J. M.; Klene, M.; Knox, J. E.; Cross, J. B.; Bakken, V.; Adamo, C.; Jaramillo, J.; Gomperts, R.; Stratmann, R. E.; Yazyev, O.; Austin, A. J.; Cammi, R.; Pomelli, C.; Ochterski, J. W.; Martin, R. L.; Morokuma, K.; Zakrzewski, V. G.; Voth, G. A.; Salvador, P.; Dannenberg, J. J.; Dapprich, S.; Daniels, A. D.; Farkas, Ö.; Foresman, J. B.; Ortiz, J. V.; Cioslowski, J.; Fox, D. J. *Gaussian 09*, revision B.01; Gaussian, Inc.: Wallingford, CT, 2010.

(42) Cancès, E.; Mennucci, B.; Tomasi, J. *J. Chem. Phys.* **1997**, *107*, 3032–3041.

(43) Mennucci, B.; Tomasi, J. *J. Chem. Phys.* **1997**, *106*, 5151–5158.

(44) Mennucci, B.; Cancès, E.; Tomasi, J. *J. Phys. Chem. B* **1997**, *101*, 10506–10517.

(45) Tomasi, J.; Mennucci, B.; Cancès, E. *J. Mol. Struct. (THEOCHEM)* **1999**, *464*, 211–226.